

# PHYSICAL REVIEW B

## CONDENSED MATTER

THIRD SERIES, VOLUME 34, NUMBER 3

1 AUGUST 1986

### Dangling bond in amorphous hydrogenated silicon: Anomalous spin relaxation

U. Vahalia, J. Ferrario,\* and E. A. Schiff†

Department of Physics, Syracuse University, Syracuse, New York 13244-1130

(Received 12 November 1985)

Spin relaxation of the dangling-bond defect in undoped plasma-deposited amorphous silicon has been studied using several electron-spin-resonance methods based on finite magnetic-field-modulation frequency effects. Spin-lattice relaxation ( $T_1$ ) processes alone do not account for the observations. Possible origins of the anomalous spin relaxation in spectral diffusion processes are discussed. Anomalous relaxation gives an additional signature of the dangling-bond defect which varies with deposition conditions. Solutions to Bloch's equations for inhomogeneous spin systems at finite magnetic-field-modulation frequency are given, and a general relationship between modulation-frequency effects in conventional ESR and electron-electron double-resonance measurements is established.

#### INTRODUCTION

The dangling-bond defect in hydrogenated amorphous silicon ( $a$ -Si:H) is the only defect observed by electron-spin resonance (ESR) in undoped  $a$ -Si:H at 300 K and above; it is thus the most plausible candidate to explain many defect-related properties of the material. Recently a surprisingly simple "standard" model invoking only the singly occupied dangling bond ( $D^0$ ) and a doubly occupied state ( $D^-$ ) lying a few tenths of an eV higher in the forbidden gap has enjoyed considerable quantitative success in accounting for deep-trapping effects in photocarrier transport<sup>1</sup> and even for the "Staebler-Wronski" effect.<sup>2</sup> Although the descriptive range of this standard model for bulk properties of  $a$ -Si:H is not fully defined, the importance of the dangling bond in  $a$ -Si:H is convincingly established.

Three properties of the dangling bond can be explored using ESR: the spectrum, the total density of dangling bonds, and spin relaxation. In  $a$ -Si:H the dangling-bond spectrum is attributed to inhomogeneous broadening by rotational averaging of an anisotropic gyromagnetic tensor and by random strain and hyperfine environments. In the comprehensive experiments of Stutzmann and Biegelsen<sup>3</sup> on dispersion-mode ESR in  $a$ -Si:H, relaxation was interpreted in terms of spin-lattice relaxation alone; the spin-lattice relaxation time  $T_1$  obtained was nearly material independent, being only slightly affected by the dangling-bond density, and at 300 K  $T_1$  was approximately 10  $\mu$ s. Although still earlier investigators using absorption-mode ESR had also concluded that spin-lattice relaxation was dominant, smaller values for  $T_1$  of the order of 1  $\mu$ s or less at 300 K had been given.<sup>4,5</sup>

In this paper we present results from a survey of dangling-bond relaxation effects in  $a$ -Si:H using both methods previously employed as well as a new technique of our own. Our measurements show that the quantitative discrepancy existing in the literature is not necessarily due to the difference between the specimens involved, but may instead be related to the different techniques employed. In particular, for a given specimen our estimates of  $T_1$  from the two conventional procedures disagree by approximately 1 order of magnitude. Related difficulties in accounting for relaxation measurements in other materials have been attributed to *spectral diffusion* processes.<sup>6,7</sup> Spectral diffusion violates the assumption that inhomogeneous broadening can be represented as a distribution of static, noninteracting *spin packets* having different gyromagnetic ratios because of differing defect orientations, strain, or nuclear hyperfine environments.

One possible mechanism for spectral diffusion in  $a$ -Si:H would be that changes in the hyperfine magnetic environment of the dangling bond occur on a time scale less than  $T_1$ . Such a change (which might be caused by a nearby nuclear spin flip) shifts the dangling bond out of resonance with the microwave field, and alters the response of the dangling-bond system to strong ("saturating") microwave magnetic fields. Similar effects are responsible for electron-nuclear double resonance (ENDOR) in  $a$ -Si:H due to "matrix" protons and <sup>29</sup>Si nuclei.<sup>8,9</sup> However, this model suggests that deuterated material,  $a$ -Si:D, would show different dangling-bond relaxation properties than  $a$ -Si:H. In fact  $a$ -Si:D appears quite similar to  $a$ -Si:H in at least one study,<sup>3</sup> and thus the origin of the effects reported here is unclear.

The present work primarily exploits the dependence of

ESR signals upon the magnetic-field-modulation frequency. In the two appendixes we discuss such effects in general. In Appendix A we give explicit solutions to Bloch's equations at finite modulation frequency for  $T_1 = T_2$ ; the calculation describes spin systems in which a well-defined spin-lattice relaxation time  $T_1$  is the only significant spin relaxation process. These solutions further illustrate our contention that  $T_1$  processes do not provide a comprehensive description of spin relaxation phenomena in  $a$ -Si:H, and they also help to establish a more general point of view—not based on Bloch's equations—regarding modulation-frequency effects. Specifically, in Appendix B we establish the close relationship between modulation-frequency effects in ESR and electron-electron double resonance (ELDOR); ELDOR is an experimental technique in which the effects of a saturating microwave field are observed upon the microwave susceptibility of the resonant system at a second microwave frequency somewhat removed from that of the saturating field. ELDOR measurements are particularly useful in probing spectral diffusion processes, and for this reason the establishment of the connection between ELDOR and conventional ESR techniques permits us to exploit the ELDOR literature in discussing our  $a$ -Si:H experiments.

### EXPERIMENTAL

Specimens for this work were prepared using rf plasma decomposition of Ar-SiH<sub>4</sub> mixtures. The reactor is a stainless-steel, "capacitive"-type and is pumped using a trapped two-stage rotary pump. The typical operating pressure of the reactor was 200 mTorr. Specimens were deposited onto heated Al foil affixed to the rf-grounded electrode; specimens were removed from the foils using nitric acid and the remaining  $a$ -Si-H powder was transferred into fused-quartz specimen tubes. ESR studies were performed using a Varian Inc. E-9 spectrometer with dispersion capability; the spectrometer was modified to permit the use of continuous magnetic-field-modulation frequencies  $\nu_m$ . It is worth noting that low-modulation-frequency dispersion-mode measurements using this spectrometer require a careful assessment of the effects of the automatic microwave-frequency control (AFC) circuit. The microwave magnetic field  $H_1$  inside the cavity was computed from the incident microwave power and the measured cavity  $Q$  and dimensions.<sup>10</sup> This calibration agreed with an independent measurement of  $H_1$  based on the broadening of the spectrum of diphenylpicrylhydrazyl (DPPH) at high  $H_1$ .

The spectra recorded were attributed to the dangling-bond (threefold-coordinated silicon) defect on the basis of the  $g$  value of 2.0055 corresponding to the peak defect response. The spectra reported here are from the low-modulation-amplitude limit in which the spectrum was proportional to the modulation amplitude  $H_m$ . This low-amplitude limit was surprisingly easy to reach; deviations from proportionality of less than 5% could be obtained for  $H_m < 0.5$  G for modulation frequencies  $\nu_m < 10$  kHz and for  $H_m < 0.2$  G at  $\nu_m = 100$  kHz. Such modulation amplitudes certainly exceed the width of the "spin packets" of which the inhomogeneous line shape is composed;

however, studies of the proportionality between our observed signal and the modulation amplitude showed no deviations from proportionality at the lowest practicable amplitudes  $H_m = 0.01$  G. Additional discussion of the wide range of linearity is given at the conclusion of Appendix B.

The most complete previous study<sup>3</sup> of dangling-bond relaxation properties in undoped  $a$ -Si:H was done using the dependence of the quadrature-detected ( $90^\circ$  out of phase), dispersion-mode ESR signal  $d_{90}$  upon the magnetic-field-modulation frequency  $\nu_m$ . For a strongly inhomogeneously broadened, saturated spin system, and assuming  $T_1 = T_2$ , the peak of the signal versus frequency curve yields  $1/2\pi T_1$ .<sup>3,11,12</sup> In Fig. 1 we illustrate our measured spectra for four levels of microwave power. These data are substantially the same as previously reported,<sup>3</sup> and apparently yield  $T_1 = 5 \mu\text{s}$ .

From the point of view of instrumental sensitivity, an easier method to obtain a relaxation time in  $a$ -Si:H at 300 K is simply to measure the dependence of the absorption ESR signal  $a_0$  upon the microwave magnetic field  $H_1$ .<sup>10</sup> The method depends on deviations of the dependence of  $a_0$  from the value  $a_{\text{lin}}$  extrapolated from the low- $H_1$  linear regime (see Fig. 2). For later discussion it is convenient to use a "hole-depth" parameter  $\lambda$  to measure the suppression of  $a_0$  due to saturation of the inhomogeneous line:

$$\lambda(H_1) = 1 - a_0/a_{\text{lin}} \quad (1)$$

The parameter  $\lambda$  is similar to the *reduction factor*  $R$  defined in the ELDOR literature.<sup>13</sup> If Bloch's equations with  $T_1 = T_2$  are valid (cf. Appendix A), then for an inhomogeneous system  $T_1$  is obtained from the value of  $H_1$  for which

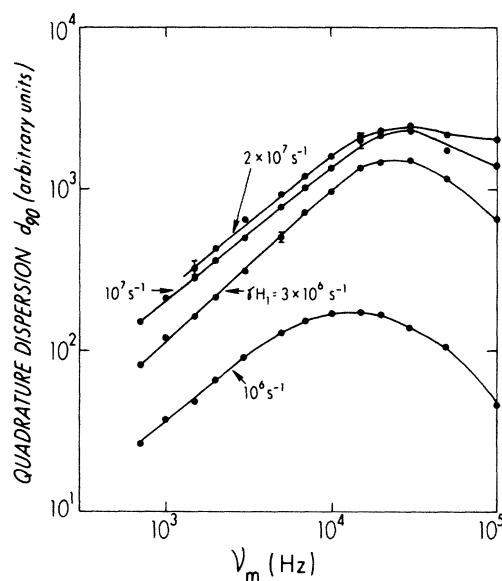


FIG. 1. Quadrature detected dispersion signal ( $d_{90}$ ) as a function of magnetic-field-modulation frequency at four microwave magnetic-field amplitudes. Specimen prepared at  $130^\circ\text{C}$  using 10% (molar) of SiH<sub>4</sub> in Ar; reactor operating at 100 kHz; spin density of specimen is  $9 \times 10^{17} \text{ cm}^{-3}$  and thickness is  $5.5 \mu\text{m}$ .

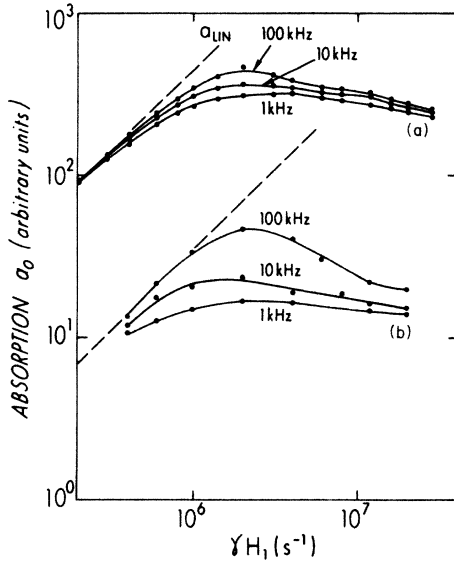


FIG. 2. In-phase detected absorption signal ( $a_0$ ) as a function of the microwave magnetic-field amplitude  $H_1$  for the specimen of Fig. 1 (a) and for an additional specimen (b) deposition temperature 260°C, using 50% SiH<sub>4</sub> in Ar, reactor operating at 13.56 MHz; spin density was  $8 \times 10^{16} \text{ cm}^{-3}$  and thickness was 11  $\mu\text{m}$ . Signals were normalized by specimen volumes.

$$\lambda(H_0/\omega T_1) = 0.3, \quad (2)$$

where  $\omega$  is the microwave frequency and  $H_0$  is the static magnetic field. In Fig. 2 we show the  $a_0$  measurements for two specimens. (a) is the specimen for the dispersion-mode data of Fig. 1, and was prepared with the reactor operating at an rf of 100 kHz. In order to permit the dispersion-mode measurements of Fig. 1 it was necessary to use a very defective specimen, but similar absorption-mode data were obtained for lower spin-density specimens prepared under the same rf conditions. The second specimen was prepared at 13.56 MHz rf frequency; again, similar data were obtained for specimens with densities varying over more than 1 order of magnitude of spin density. Data are displayed at several modulation frequencies; to obtain an estimate of the relaxation time using the hole-depth approach described above it is necessary to operate in the limit of low  $\nu_m$ .

The absorption-mode data for the 100 kHz rf specimen yield a relaxation time of 0.7  $\mu\text{s}$ , approximately an order of magnitude shorter than the dispersion-mode estimate for the same specimen. The estimate for the lower-spin-density specimen (b) is 1.6  $\mu\text{s}$ . The frequency dependence of the saturation curves for this specimen is surprising given this estimate for  $T_1$ . Because the observed signal is proportional to the magnetic-field-modulation amplitude, we rule out the possibility that the enhancement of signal at higher frequencies is simply due to reduction of the extent of spin-packet saturation due to rapid passage through the packet's resonance.

The discrepancy between "modulation-frequency-resolved" estimates of the spin relaxation rate and those obtained using steady-state saturation is presented more clearly in Fig. 3, in which the measured hole depth  $\lambda$  is

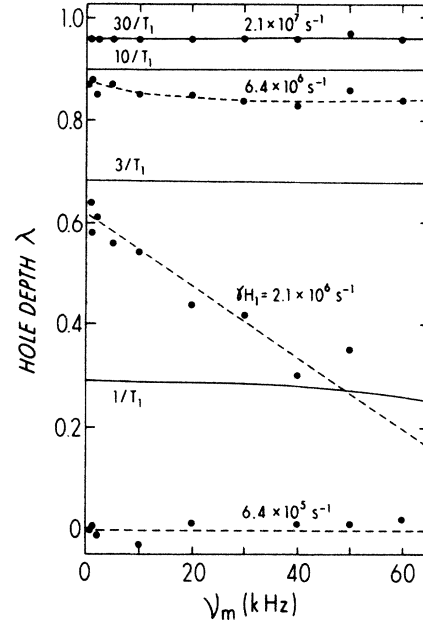


FIG. 3. Hole-burning parameter  $\lambda$  as a function of magnetic-field-modulation frequency. Theoretical curves (solid lines) are obtained by direct solution of Bloch's equations for an inhomogeneous spin system using  $T_1 = T_2 = 1.6 \mu\text{s}$  in Eq. (A3) from the text. The labels of these curves indicate the values of  $\gamma H_1$  in units of  $T_1^{-1}$ . Experimental points are for specimen (b) (cf. Fig. 2); the dashed lines are simply smooth curves through the experimental data for the specified values of  $\gamma H_1$ .

plotted as a function of modulation frequency for several levels of the microwave magnetic field  $\gamma H_1$ ; the dashed lines are simply smooth curves through this data. The continuous lines are theoretical curves obtained from the  $T_1 = T_2$  solutions to Bloch's equations for inhomogeneous spin systems and small modulation amplitude; the preparation of this family of theory curves requires knowledge of  $T_1$ , which was set to 1.6  $\mu\text{s}$  using the procedure of Eq. (2). The theoretical curves exhibit essentially no frequency dependence, in contrast to the experimental behavior. This figure demonstrates that Bloch's equations do not account for absorption-mode relaxation for our specimens of *a*-Si:H; we could not account for the data of Fig. 3 within Bloch's equations either by relaxing the  $T_1 = T_2$  assumption or by invoking spin subsystems with differing relaxation properties.

## DISCUSSION

Figure 3 can be given a simple physical interpretation in terms of electron-electron double-resonance experiments.<sup>6,7,13</sup> In ELDOR a weak probe is applied at one microwave frequency while a stronger, "hole-burning" microwave field is applied at a nearby frequency. From this point of view Fig. 3 displays the effects upon the absorption-mode signal of a hole-burning field separated in frequency by  $\nu_m$  from the probe. The similarity between ELDOR and modulation-frequency experiments originates in the equivalence of magnetic-field modulation of the spin system and frequency modulation of the microwaves. Frequency modulation generates sidebands

separated by the modulation frequency from the carrier, and is an alternate experimental implementation of ELDOR; the primary difference between ELDOR and magnetic-field-modulation experiments lies in the differing microwave detection schemes. The relationship between ELDOR and magnetic-field modulation is discussed further in Appendix B. An example of the value of the ELDOR interpretation of magnetic-field-modulation experiments is that it explains in a natural way the otherwise surprising fact that low- $H_1$  (unsaturated) measurements are unaffected by modulation frequencies exceeding  $1/T_1$ . In the ELDOR point of view a sufficiently weak "hole-burning" field does not affect the sample's response to the probe field.

Anomalous relaxation has been studied in several materials using ELDOR techniques, including the  $F$ -center defect in KCl (Ref. 6) and trapped electrons in aqueous glasses.<sup>7</sup> In these two cases magnetic nuclei proved to be the origin of the anomalies. The magnetic nuclei give rise to spectral diffusion processes because they generate a local magnetic field which can fluctuate on the time scale of spin-lattice relaxation. It should be noted that conventional nuclear magnetic resonance relaxation does not directly address the problem of relaxation of a coupled magnetic nucleus and paramagnetic defect; this problem has been addressed with some success by phenomenological models.<sup>13</sup> The case of trapped electrons in aqueous glass is illustrative of the possible role of magnetic nuclei; protons were identified as the origin of the anomalous relaxation by a careful comparison of ELDOR observations in deuterated and protonated material. Relaxation in the deuterated material could be understood using the conventional spin-packet approach. Interestingly, the absolute differences in relaxation-time estimates between the deuterated and protonated material were not large.

In  $\alpha$ -Si:H studies of relaxation using magnetic-field-modulation effects upon dispersion mode give essentially the same results for  $\alpha$ -Si:H and  $\alpha$ -Si:D.<sup>3</sup> Although more complete relaxation studies would be desirable, this work indicates that magnetic nuclei may not be important in spin relaxation for  $\alpha$ -Si:H. The principal alternate spectral diffusion mechanism appropriate for a dilute paramagnetic system such as  $\alpha$ -Si:H is actual motion of the defect, either as tunneling between similar sites or diffusion. Additional experimental work is required to determine the origins of anomalous relaxation in  $\alpha$ -Si:H and the utility of ELDOR signature information as a description of the dangling-bond's configuration.

#### ACKNOWLEDGMENTS

The authors thank A. Honig for many illuminating conversations, R. Pandya for specimens, and S. Zafar for assistance. This research was supported by the National Science Foundation through Grant No. DMR 83-06083.

#### APPENDIX A: SOLUTIONS TO BLOCH'S EQUATIONS FOR INHOMOGENEOUS SPIN SYSTEMS AT ARBITRARY MODULATION FREQUENCY

The effects of magnetic-field modulation at finite modulation frequency upon ESR have been extensively

examined in the literature because of the utility of this approach in exploring spin relaxation phenomena. The most recent work on "saturation transfer spectroscopy" is primarily directed at understanding the consequences of rotational diffusion, but it incorporates the earlier work in other contexts, and the reader is referred to Ref. 14 for an extended review of the technique. The customary point of departure in efforts to account for spin relaxation phenomena is Bloch's equations, and in this appendix we first review the solutions to these equations obtained with the following conditions: (i) The "single-spin" solutions for which  $T_1 = T_2$  and (ii) small modulation amplitude. The  $T_1 = T_2$  assumption is reasonable for dilute paramagnetic systems such as defects in semiconductors. To apply the solutions it is usually necessary to take into account the inhomogeneity of the spin system. Neglecting spectral diffusion processes, an inhomogeneous signal  $S_{\text{inh}}(H)$  is obtained from the corresponding homogeneous solution  $S_{\text{hom}}(h)$  by convolution with an envelope function  $\epsilon(H)$ :

$$S_{\text{inh}}(H) = \int_{-\infty}^{\infty} d\tilde{H} S_{\text{hom}}(H - \tilde{H}) \epsilon(\tilde{H}). \quad (\text{A1})$$

This expression assumes that inhomogeneity affects only the resonant fields of otherwise identical spin packets.

We consider the solutions to Bloch's equations with microwave magnetic field  $H_1 \cos(\omega t)$  and amplitude-modulated magnetic field  $H_0 + H_m \cos(\omega_m t)$ ; the signals detected in a magnetic-field-modulation spectrometer are the modulated components of the microwave magnetization. We introduce the following dimensionless variables: the modulation frequency,  $Z_m = \omega_m T$ ; the microwave amplitude,  $Z_1 = \gamma H_1 T$ ; the magnetic field,  $h = \gamma(H - H_0)T$ ; the modulation amplitude;  $A_m = \gamma H_m T$ ; and the saturation factor,  $S_d = 1 + Z_1^2 - Z_m^2$ , where  $H_0 = \omega/\gamma$ , and  $\gamma$  is the spin system's gyromagnetic ratio. Solving Bloch's equations for the sinusoidal absorption magnetization

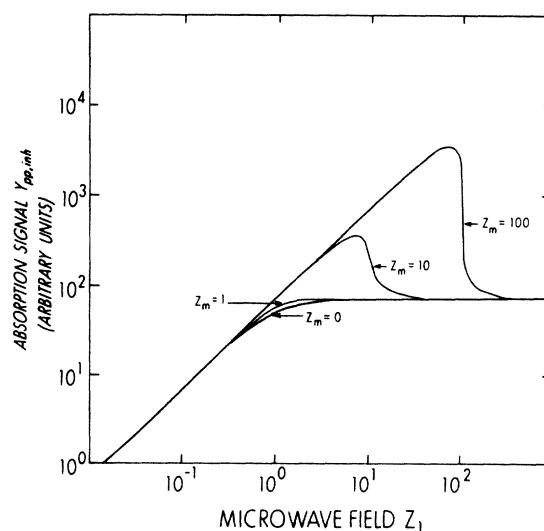


FIG. 4. Absorption magnetization  $Y_{\text{inh}}$  of an inhomogeneous spin system detected in-phase with magnetic-field modulation as computed from Bloch's equations [Eq. (A3) of the text].  $Y_{\text{inh}}$  is plotted as a function of the normalized microwave amplitude  $Z_1 = \gamma H_1$  for several modulation frequencies  $Z_m = \omega_m T_1$ .

response in phase with the magnetic-field modulation we obtain

$$Y_{\text{hom}}(H) = \frac{4Z_1 A_m M_0 h}{(S_d + h^2)^2 + 4Z_m^2}, \quad (\text{A2})$$

where  $M_0$  is the nonresonant magnetization of the spin-packet  $\chi_0 H$ .

These homogeneous solutions must be integrated over an envelope of spin-packet  $g$  values to obtain the spectrometer's response in an inhomogeneous spin system. For extreme inhomogeneous broadening the envelope function may be replaced by its power-series expansion. The lowest term in the resulting expansion is zero, since  $\int dh Y_{\text{hom}}(h) = 0$ . The first nonzero term can be evaluated using contour integration, and we obtain

$$Y_{\text{inh}}(H) = \epsilon'(H) \frac{Z_1 A_m}{[S_d + (S_d^2 + 4Z_m^2)^{1/2}]^{1/2}}, \quad (\text{A3})$$

$$X_{\text{hom}}(h) = \frac{2Z_1 Z_m A_m M_0 [(3 + 3Z_m^2 - Z_1^2)h^2 - S_d^2 - 4Z_m^2]}{(1 + Z_m^2)(1 + Z_1^2 + h^2)[(S_d + h^2)^2 + 4Z_m^2]}. \quad (\text{A4})$$

This complex expression generates a fairly simple curve which will be discussed further in Appendix B. The inhomogeneous expression is still more complex:

$$X_{\text{inh}} \propto \frac{K\{1 + [2(S + K)/(1 + Z_1^2)]^{1/2}\} - 3(1 + Z_m^2) + Z_1^2}{(1 + Z_m^2)(S + K)\{1 + Z_1^2 + K + [2(S + K)(1 + Z_1^2)]^{1/2}\}}, \quad (\text{A5})$$

where  $K = (S^2 + 4Z_m^2)^{1/2}$ ,  $S = 1 + Z_1^2$ , and the proportionality constant is  $A_m Z_1 Z_m \epsilon(H)$ . These dispersion expressions are important in light of their relationship to the method of obtaining  $T_1$  from the peak  $d_{90}$  signal as a function of modulation frequency under conditions of saturation of the resonance.<sup>11,12</sup>  $X_{\text{inh}}$  has been plotted as a function of modulation frequency in Fig. 5. The method

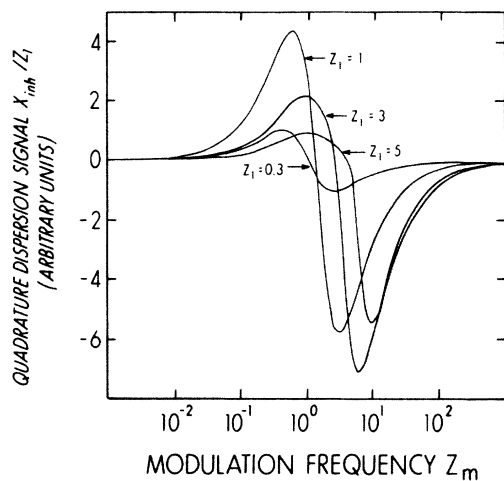


FIG. 5. Dispersion magnetization  $X_{\text{inh}}$  of a very inhomogeneous spin system derived from Bloch's equations [cf. expression (A5) of the text] for detection in quadrature with magnetic-field modulation.  $X_{\text{inh}}$  is plotted as a function of normalized modulation frequency  $Z_m = \omega_m T_1$  for several microwave amplitudes  $Z_1 = \gamma H_1$ .

where in utilizing this expression  $\gamma = \omega/H$ .

These magnetization expressions are proportional to the spectrometer signal  $a_0$ , and Eq. (A3) was used to prepare the theoretical curves of Fig. 3. In Fig. 4  $a_0$  is plotted as a function of  $Z_1$  for various  $Z_m$ . The solutions for low microwave magnetic field are independent of modulation frequency even when this frequency exceeds  $1/T_1$ ; the homogeneous solutions, on the other hand, depend strongly upon  $Z_m$  in this regime. This result means that low- $H_1$  spin-density measurements are valid even for large modulation frequencies ( $Z_1 > 1$ ). At least for  $a$ -Si:H, this useful feature is often exploited in spin-density determinations without discussion. The result is a straightforward consequence of the ELDOR analogy discussed in Appendix B.

The expressions for dispersion magnetizations detected in quadrature with the modulation are obtained by the same procedures used for absorption. The results are

(which was based on the approximate calculation of Portis<sup>11</sup>) agrees with solutions of Bloch's equations. However, these solutions also predict another feature: a sign reversal at sufficiently high modulation frequency, where  $Z_1 = Z_m$ . This feature is the *rotary saturation* of Redfield<sup>15</sup> (see also Ref. 16).

## APPENDIX B: ELDOR AND MAGNETIC-FIELD-MODULATION ESR

The close relationship between the effects of changes in the longitudinal magnetic field and of changes in the microwave frequency of a spin resonance experiment is evident from the resonance relationship  $\omega = \gamma H$ . The equivalence of modulation of the microwave frequency (fm) and of amplitude modulation of the magnetic field is easily shown by Bloch's equations, and this equivalence also appears to be generally valid.<sup>17</sup> This equivalence permits prediction of several features of the solutions to Bloch's equations through examination of the consequences of fm, and it also reveals the close correspondence of absorption-mode ESR with finite modulation frequency and ELDOR.

Consider the magnetization expected for a frequency modulated microwave source:

$$\omega(t) = \omega + (\delta\omega)\cos(\omega_m t).$$

For small frequency excursions  $\delta\omega$ , the resulting microwave field has two opposing sidebands:

$$H_1(t) = H_1(\cos(\omega t) + (\delta\omega/2\omega_m)\{\cos[(\omega + \omega_m)t] - \cos[(\omega - \omega_m)t]\}) .$$

Three transverse magnetizations result from this field. In complex notation and using complex susceptibilities at the three frequencies  $\omega - \omega_m$ ,  $\omega$ ,  $\omega + \omega_m$ :

$$\tilde{M}(t) = H_1\{\tilde{\chi}e^{i\omega t} + (\delta\omega/2\omega_m)[\tilde{\chi}_+e^{i(\omega + \omega_m)t} - \tilde{\chi}_-e^{-i(\omega - \omega_m)t}]\} .$$

The magnetization in the frame rotating at the instantaneous frequency  $\omega(t)$  has four sinusoidal components representing the four spectrometer signals.

Absorption, in-phase:

$$(\chi''_+ - \chi''_-)(H_1\delta\omega/2\omega_m) . \quad (\text{B1a})$$

Absorption, quadrature:

$$(2\chi' - \chi'_+ - \chi'_-)(H_1\delta\omega/2\omega_m) . \quad (\text{B1b})$$

Dispersion, in-phase:

$$(\chi'_+ - \chi'_-)(H_1\delta\omega/2\omega_m) . \quad (\text{B1c})$$

Dispersion, quadrature:

$$(2\chi'' - \chi''_+ - \chi''_-)(H_1\delta\omega/2\omega_m) . \quad (\text{B1d})$$

The customary notation  $\tilde{\chi} = \chi' + i\chi''$  has been used. It is important to note that  $\tilde{\chi}$  is a large-signal susceptibility, whereas  $\tilde{\chi}_+$  and  $\tilde{\chi}_-$  are incremental (small signal) susceptibilities. These expressions explain the primary features of the solutions to Bloch's equations given in Appendix A. Figure 6 shows the results of computations for the  $a_0$  and  $d_{90}$  signals from expressions (A2) and (A4) of Appendix A in the limit of small  $H_1$  (where the distinction between small- and large-signal susceptibilities is unimportant). For both cases the computations agree with the expectations from the fm expressions (B1a)–(B1d), and in particular for large modulation frequency  $Z_m$  the signals consist of separated components which can readily be identified with the terms of these expressions.

The correspondence between ELDOR and frequency modulation for inhomogeneous spin systems is easily demonstrated. In ELDOR the susceptibility  $\chi''_+$  is directly measured using a probe microwave field. In the fm experiment a general expression for the relationship of  $\chi_+$  and  $\chi_-$  can be obtained in terms of the slowly varying, inhomogeneous envelope function  $\epsilon(\omega)$ :

$$\tilde{\chi}_+/\epsilon(\omega + \omega_m) = \tilde{\chi}_-/\epsilon(\omega - \omega_m) . \quad (\text{B2})$$

Note that  $\tilde{\chi}$  itself need not be (and is not) slowly varying. Exploiting this relationship in evaluating the  $a_0$  signal from expression (B1a) we obtain

$$a_0 \propto \chi''_+ - \chi''_- = \chi''_+[2\omega_m\epsilon'(\omega)/\epsilon(\omega)] . \quad (\text{B3})$$

Hence, ELDOR and the fm response are both proportional to  $\chi''_+$ , the incremental absorption susceptibility at a frequency  $\omega_m$  away from the main, "hole-burning" microwave field at  $\omega$ .

The ELDOR correspondence of expression (B3) was derived for the small modulation amplitude limit

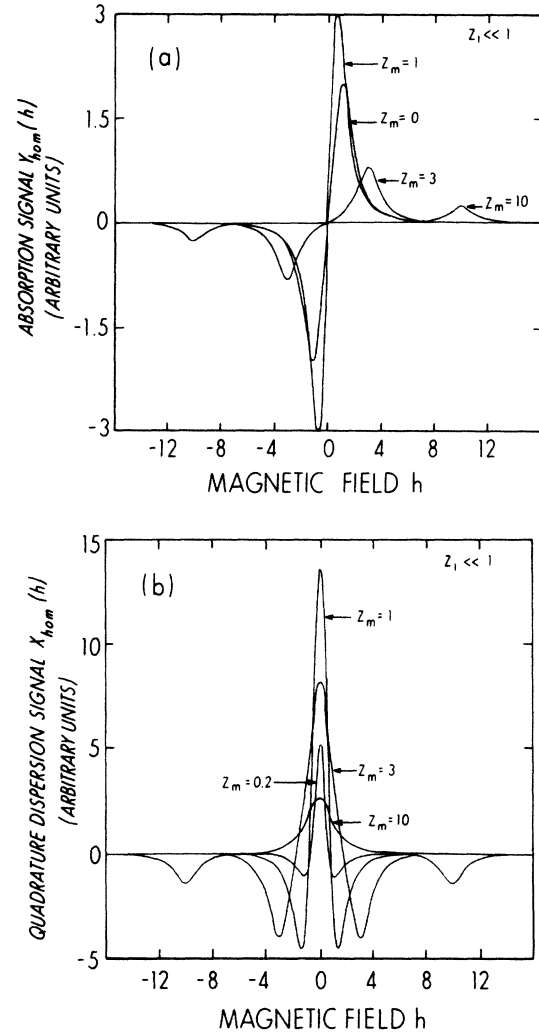


FIG. 6. (a) In-phase absorption magnetization  $Y_{\text{hom}}$  and (b) quadrature dispersion magnetization  $X_{\text{hom}}$  derived from Bloch's equations for a homogeneous spin system with magnetic-field modulation and small microwave fields. The magnetizations are plotted as a function of the deviation  $h = \gamma(H - H_0)T_1$  from the spin's resonant field  $H_0$  for several modulation frequencies  $Z_m = \omega_m T_1$ . The curves can be understood in terms of the more general sideband argument given in the text.

$\delta\omega/\delta\omega_m = \gamma H_m/\omega_m \ll 1$ . One might reasonably expect that the proportionality of the signal to  $H_m$  would break down when this inequality is violated by experimental conditions, and the simple ELDOR scheme outlined here to become useless. In fact the assumption  $\delta\omega/\omega_m \ll 1$  appears to be more convenient than appropriate as a criterion for the breakdown of the ELDOR correspondence. For example, for small  $\omega_m$  the signal is obviously proportional to  $H_m$  subject to the much weaker restriction that  $H_m$  be smaller than the *inhomogeneous* envelope width. Thus despite the fact that the sideband distribution is not simple for  $\delta\omega/\delta\omega_m > 1$  the susceptibility obtained after summation over the sidebands is the same as that obtained by considering small modulation index  $\delta\omega/\omega_m$  and a single pair of sidebands. A similar result was obtained by

Halbach<sup>17</sup> for  $H_1$  nonsaturating: for sufficiently inhomogeneous lines, the signal is strictly proportional to  $H_m$  even for  $\delta\omega/\omega_m > 1$ . This result was obtained from explicit summation over multiple sidebands. Thus the ELDOR analogy proposed here provides a satisfactory

description of ESR on inhomogeneous systems well beyond the limits of our derivation. A more general treatment from which the breakdown of the proportionality between the signal and  $H_m$  could be predicted for inhomogeneous lines would of course be desirable.

---

\*Present address: IBM Research Laboratories, Poughkeepsie, NY.

†Address correspondence to this author.

<sup>1</sup>R. A. Street, *Philos. Mag.* **B 49**, L15 (1984).

<sup>2</sup>M. Stutzmann, W. B. Jackson, and C. C. Tsai, *Phys. Rev. B* **32**, 23 (1985).

<sup>3</sup>M. Stutzmann and D. Biegelsen, *Phys. Rev. B* **28**, 6236 (1983).

<sup>4</sup>S. Hasegawa and S. Yazaki, *Thin Solid Films* **55**, 15 (1978).

<sup>5</sup>P. J. Gaczi and D. Booth, *Solar Energy Materials* **4**, 279 (1981).

<sup>6</sup>P. R. Moran, *Phys. Rev.* **135**, A247 (1964).

<sup>7</sup>D. P. Lin and L. Kevan, *J. Phys. Chem.* **81**, 966 (1977).

<sup>8</sup>S. Yamasaki, S. Kuroda, J. Isoya, H. Okushi, and K. Tanaka, *J. Non-Cryst. Solids* **77/78**, 727 (1985).

<sup>9</sup>M. Stutzmann, *Phys. Rev. B* **33**, 7379 (1986); M. Stutzmann and D. K. Biegelsen (unpublished).

<sup>10</sup>C. P. Poole, *Electron Spin Resonance*, 2nd ed. (Wiley, New York, 1983).

<sup>11</sup>A. M. Portis (unpublished).

<sup>12</sup>C. A. J. Amerlaan and A. Van der Wiel, *J. Magn. Reson.* **21**, 387 (1976).

<sup>13</sup>L. Kevan and P. A. Narayana, in *Multiple Electron Resonance Spectroscopy*, edited by M. M. Dorio and J. H. Freed (Plenum, New York, 1979), p. 229.

<sup>14</sup>J. S. Hyde and L. R. Dalton, in *Spin Labeling II: Theory and Applications*, edited by Lawrence J. Berlin (Academic, New York, 1979).

<sup>15</sup>A. G. Redfield, *Phys. Rev.* **98**, 1787 (1955).

<sup>16</sup>A. Abragam, *The Principles of Nuclear Magnetism* (Oxford University, New York, 1961).

<sup>17</sup>K. Halbach, *Phys. Rev.* **119**, 1230 (1962).